bioRxiv preprint doi: https://doi.org/10.1101/2020.11.24.396051; this version posted November 24, 2020. The copyright holder for this preprint (which was not certified by peer review) is the author/funder, who has granted bioRxiv a license to display the preprint in perpetuity. It is made available under aCC-BY-NC-ND 4.0 International license.

GLYCOLIC ACID PROTECTS NEURONS AGAINST ISCHEMIA *IN VITRO* AND IN TWO ANIMAL MODELS OF STROKE

Alexandra Chovsepian*[1] Daniel Berchtold*[2], Katarzyna Winek*[2, ¶], Uta Mamrak[3], Inés Ramírez Álvarez[4,5,‡], Yanina Dening[1], Luis Weitbrecht[2], Claudia Dames[2], Marine Aillery[1,+], Celia Fernandez-Sanz[4,5,†], Marianne Dieterich[4,5], Peter Falkai[2], Nikolaus Plesnila[3,5], Andreas Meisel[2], Francisco Pan-Montojo[1,4,5,Ψ]

[1] Department of Psychiatry, Ludwig-Maximilian University, Nußbaumstrasse. 7, 80336 Munich, Germany

[2] Department of Neurology, NeuroCure Clinical Research Center, Center for Stroke Research, Charité University Medicine, Charitéplatz 1, 10117 Berlin, Germany

[3] Laboratory of Experimental Stroke Research, Institute for Stroke and Dementia Research (ISD), University of Munich Medical Center, Feodor-Lynen-Strasse 17, 81377 Munich, Germany

[4] Department of Neurology, Ludwig-Maximilian University, Marchioninstrasse. 15, 81377 Munich

[5] Munich Cluster for Systems Neurology (SyNergy), Ludwig-Maximilian University Munich, Germany

[*] These authors contributed equally to this work.

[¶] Present address: Edmond and Lily Safra Center for Brain Sciences, Hebrew University of Jerusalem, Israel

[+] Present address: Seppic, La Garenne-Colombes, Île-de-France, France

[†] Present address**:** Center for Translational Medicine, Department of Medicine, Thomas Jefferson University, Philadelphia, PA 19107, USA

[Ψ] Corresponding author. Email: Francisco.Pan-Montojo@med.uni-muenchen.de

ABSTRACT

Stroke is the second leading cause of death and disability worldwide. Current treatments, like pharmacological thrombolysis or mechanical thrombectomy, re-open occluded arteries but do not protect against ischemia-induced damage caused before reperfusion or ischemia/reperfusion- induced neuronal damage. It has been shown that knocking out *djr-1.1 and djr-1.2* or *glod-4* results in a decreased tolerance to anhydrobiosis in *C elegans* dauer larva and that Glycolic Acid (GA) can rescue this phenotype. During the process of desiccation/rehydration, a metabolic stop/start similar to the one observed during ischemia/reperfusion occurs. In this study we tested the protective effect of GA against ischemia in three different models (oxygen-glucose deprivation *in vitro* and Global cerebral ischemia as well as Middle Cerebral Artery Occlusion *in vivo*). Our results show that GA, given during reperfusion, strongly protects against ischemia-

bioRxiv preprint doi: https://doi.org/10.1101/2020.11.24.396051; this version posted November 24, 2020. The copyright holder for this preprint (which was not certified by peer review) is the author/funder, who has granted bioRxiv a license to display the preprint in perpetuity. It is made available under aCC-BY-NC-ND 4.0 International license.

induced neuronal death, reduces the mortality in mice with large infarcts, significantly reduces the ischemic area in the brain and improves the functional outcome. The effect of GA is stronger when the substance is applied near the damaged tissue (i.e. directly to the neurons *in vitro* or intra-arterially via the internal carotid artery *in vivo*). These results suggest that GA treatment has the potential to dramatically reduce the mortality and disability caused by stroke in patients.

INTRODUCTION

Stroke is the second leading cause of death and disability worldwide, with a prevalence of 80.1 million patients, responsible for approximately 5.5 million deaths and 116.4 million disability-adjusted life years globally [1]. Ischemic stroke comprises 87% of all stroke cases [2] and is caused by a thrombotic or embolic vessel occlusion resulting in focal cerebral ischemia. It only takes minutes for the affected area to become irreversibly damaged, often resulting in long-term neurological deficits (50-60% of stroke patients [3]). The tissue surrounding the necrotic infarct core, called penumbra, receives reduced blood flow, but in more tolerable levels due to collateral perfusion and is therefore salvable [4]. The penumbra is thus the main target of current treatment strategies [5].

Several therapeutic targets have been tested after stroke, such as NMDA antagonists- [6], free radical scavengers- [7] [8] or immunomodulators (TNFa - [9], IL10 - [10]). However, all failed in the preclinical or clinical phase. The only exception is Edaravone, a radical scavenger, which received clinically approval in Japan [11]. Hence, the identification of novel neuroprotective compounds is essential for improving treatment options in ischemic stroke.

The inherent ability of *Caenorhabditis elegans* (C. elegans) to tolerate extreme desiccation could have interesting implications in stroke. The survival strategies of the C. elegans dauer larva in anhydrous conditions (desiccation) has been extensively studied [12] [13] [14] [15]. Desiccation is a form of metabolic stress (metabolic stop/start) [16] that parallelizes the metabolic halt and reactivation occurring during ischemia-reperfusion damage due to restriction of blood flow, oxygen and nutrients [17] [18] followed by an abrupt re-initiation of metabolic activity during rehydration/reperfusion. It has been shown that dauer larva strongly upregulate *djr-1.1, djr-1.2* and *glod-4* during preparation for desiccation and that these genes are crucial for desiccation tolerance [14] [19] [15]. *djr-1.1* and *djr-1.2* are orthologs of the Parkinson's disease-associated glyoxalase DJ1 (locus PARK 7) that is known to convert the reactive

bioRxiv preprint doi: https://doi.org/10.1101/2020.11.24.396051; this version posted November 24, 2020. The copyright holder for this preprint (which was not certified by peer review) is the author/funder, who has granted bioRxiv a license to display the preprint in perpetuity. It is made available under aCC-BY-NC-ND 4.0 International license.

aldehydes glyoxal and methylglyoxal to glycolic acid (GA) and D-lactic acid (DL), respectively [20] [21]. In a previous study [19], it was shown that mutant worms completely missing glyoxalase activity (i.e. lacking *djr* and *glod-4* genes) were less likely to survive desiccation. Moreover, mitochondria of *djr-1.1*; *djr-1.2* double mutant larvae and DJ1-knockdown HeLa cells showed defects in their network structure and membrane potential. These phenotypes were rescued by GA and DL which demonstrates that the aforementioned deficits are not just a result of accumulation of toxic aldehydes, but are also caused by the absence of the DJ1-glyoxalase activity products GA and DL themselves [19].

Based on these interesting results and the similarity between desiccation and ischemia-reperfusion damage [16] [17] [18], we hypothesized that GA and DL may be protective after ischemic stroke. For that purpose, we tested these substances in *in vitro* (oxygen-glucose deprivation-OGD) and *in vivo* (Global Ischemia and Middle Cerebral Artery Occlusion-MCAo) models of stroke. Overall, our results show that GA treatment exerts a powerful protection against ischemia, improvingthe functional outcome.

METHODS

In vitro hypoxia

To simulate ischemia/reperfusion (IR) *in vitro*, primary cortical neurons from E15.5 mice embryos were prepared and plated in 2 x 96-well-plates (one for normoxia and one for evaluation of necrosis with DRAQ5 and PI 30 min. post-OGD or, alternatively, one for normoxia and one for evaluation of survival with NeuN 72 hours after OGD). Plates were coated with PLL 10 µg per well in 100 µl H20, and neurons were plated at a concentration of 1x10^6 in Neurobasal A media containing 5% B27, Pen-Strep and L-glutamine (all from Life Technologies, USA) as previously described [22]. On day *in vitro* (DIV) 6, neurons were placed within the anoxic atmosphere and incubated in a N2-filled gas chamber for 1 h with glucose-free acidic anoxic buffer (previously deoxygenated in an autoclave and bubbled with N2 for 20 min) containing (in mmol/l): 140 NaCl, 3.6 KCl, 1.2 MgSO4, 1 CaCl2, 20 HEPES, pH 6.4, and supplemented with 4 µmol/l resazurin, 100 µmol/l ascorbic acid, 0.5 mmol/l dithionite and 100 U/ml superoxide dismutase. For mimicking reperfusion, the anoxic buffer was washed out and substitute by Neurobasal A media as above but without phenol red and without antioxidants (pH 7.4, Life Technologies, USA) supplemented with GA (stock solution 3,92 M diluted in water, pH adjusted to 7 with NaOH, final concentration 10 and 20 mM, Sigma, Germany) or vehicle (ddH2O). For the normoxic group, media was changed with Neurobasal A media without phenol red and without antioxidants (Life Technologies, USA), and neurons were kept in at 5% Co2, 37

bioRxiv preprint doi: https://doi.org/10.1101/2020.11.24.396051; this version posted November 24, 2020. The copyright holder for this preprint (which was not certified by peer review) is the author/funder, who has granted bioRxiv a license to display the preprint in perpetuity. It is made available under aCC-BY-NC-ND 4.0 International license.

ºC for 1 h with. 1 hour after reperfusion the volume in the well was doubled. Half of the plates were fixed with 2% PFA 30 min. after the OGD/normoxia and the other half was left in the incubator for 72 hours before fixation. Like this, it was ensured that neurons had undergone the same OGD conditions.

Cell immunofluorescence and quantification OGD

For the evaluation of necrosis, cells were fixed as mentioned above 30 min. post-OGD/normoxia. Neurons were incubated with DRAQ5 (62251, 1:10000, Thermo Fischer Scientific, MA, USA) and PI (81845, end concentration 5 µM, Sigma-Aldrich, Germany) both diluted in PBS for 5 min at room temperature, followed by aspiration and 3x PBS rinsing. Neurons were imaged using Opera High-Content Screening System (20x Air, DRAQ5: Ex. 640, Em: 690/50 nm; PI: Ex: 561, Em: 600/40, PerkinElmer, MA USA). 10 fields/well were imaged and the number of $DRAQ5^+$ and PI^+ neurons were quantified using Image J software (National Institutes of Health, Bethesda, MD) in a semi-automated manner.

For the quantification of surviving neurons, at 72 hours post- OGD/normoxia cells were fixed with 2%PFA for 35 min at room temperature or overnight at 4°C. Cells were then incubated at RT with Block solution (5%Donkey serum, 0,05% TRITON, PBS) for 1 hour. Primary antibody (NeuN Polyclonal, ab104224, Abcam, USA) was added in block solution (1:1000 dilution) for 1hour incubation at RT followed by overnight incubation at 4°C. The next day cells were washed 3 times (10 min.) with PBS and then incubated with the secondary antibody solution (AlexaFluor 555 a31570 Thermo Fisher Scientific, MA, USA, 1:500 in blocking buffer) for 2 hours at RT protected from light. After 3 washings with PBS, the cells were ready for observation. Microscopy images were obtained with an Opera High-Content Screening System (20x Air, Ex: 488 nm, Em: 568, PerkinElmer, MA USA). 10 fields/well were imaged and the number of $NeuN^+$ neurons were quantified using Image J software (National Institutes of Health, Bethesda, MD) in a semi-automated manner.

MCAo mouse model

MCAo operation:

Transient (60 min.) MCAo was performed according to a standard protocol [23]. This process creates a brain infarction in the MCA area and the resulting infarct includes broad damage in the striatum and ipsilateral cerebral cortex, as well as the presence of a relatively small penumbral area in the cortex [24]. 40 12-week-old C57Bl6/J mice underwent MCAo surgery (18 treated

bioRxiv preprint doi: https://doi.org/10.1101/2020.11.24.396051; this version posted November 24, 2020. The copyright holder for this preprint (which was not certified by peer review) is the author/funder, who has granted bioRxiv a license to display the preprint in perpetuity. It is made available under aCC-BY-NC-ND 4.0 International license.

with GA and 16 with vehicle) while 6 mice received sham surgery and GA treatment. Animals were randomly allocated to different treatment MCAo groups or the sham group. Anesthesia was induced with 2,5% isoflurane (Forene, Abbott, Wiesbaden Germany) in 1:2 Oxygen/Nitrous oxide mixture and maintained at 1.0%-1.5% throughout the operation. A 0.19 ± 0.01 mm diameter silicon rubber-coated monofilament (n°701956PK5Re Doccol Corporation, Sharon, MA, USA) was inserted in the common carotid artery and then advanced until reaching the MCA origin, where it remained for 60 min. while the mouse was allowed to recover from anaesthesia inside a heated cage for body temperature maintenance at 37°C. At the end of the 60 min. of MCA occlusion, the mouse was re-anaesthetized, the filament was gently retracted and the internal carotid artery underwent permanent ligation. For sham operation the same process was followed but the filament was removed directly after reaching the MCAo origin. For post-surgical pain prevention, Bupivacain gel (1%) was topically applied on the wound and the mouse received 500 µl saline subcutaneously for rehydration. Operated mice were placed in a heated cage for one hour before return to their home cages. Soaked food and pellets were provided post- operation in the recovery phase.

Substance preparation for i.p. administration:

100 µl of GA or 0,9 % NaCl solution were injected i.p. after the surgery till day three after MCAo/sham operation. For the GA solution, Glycolic acid powder (Glycolic Acid, Sigma Aldrich) was diluted in pure water to obtain a final concentration 15.6 mg/mL (60 mg/kg) for the intraperitoneal injection. The pH was adjusted to 7 with NaOH.

Tissue fixation and processing:

Mice were perfused 14days post MCAo. Mice were deeply anesthetized with Ketamin/Xylazin (150mg/kg and 15mg/kg respectively) and upon complete loss of pedal reflexes, transcardially perfused with 0.1M PBS solution. Brains were carefully extracted and kept in 4% PFA in a 15 ml Falcon tube overnight at 4°C. On the next day, brains were incubated in 30% sucrose until sinking, for cryoprotection. The brains were then frozen using the n-Butanol procedure. 10 ml of n-Butanol were added in a 15 ml Falcon tube and cooled down in liquid nitrogen to -50 °C. Once this temperature was reached the brains were inserted in the falcon tube which was kept in liquid nitrogen to cool down to -80°C for one minute. The brains were then ready for immediate storage in -80°C. Deeply frozen brain tissue was mounted on the sliding microtome (Leica SM210R) using OCT Tissue-Tek (Sakura Finetek Europe B.V., NL) and kept frozen with addition of dry ice for cutting. 60µm-thick sequential sections were acquired and transferred

bioRxiv preprint doi: https://doi.org/10.1101/2020.11.24.396051; this version posted November 24, 2020. The copyright holder for this preprint (which was not certified by peer review) is the author/funder, who has granted bioRxiv a license to display the preprint in perpetuity. It is made available under aCC-BY-NC-ND 4.0 International license.

sequentially in 96-well plates filled with freezing medium (50% PBS, 25% Glycerol, 25% Ethylene Glycol) for further storage at -20°C.

Staining of brain sections:

NeuroTrace staining for histological definition of lesion volume and NeuN staining were performed for quantification of surviving neurons. On staining day 1, sections were washed with PBS (pH=7.4) 3x 10 min and then incubated with blocking buffer (5% donkey serum, 0.1%Triton-X in PBS) for 1hour, under room temperature. Following that, the primary antibody (rabbit anti-NeuN, ABN78 Sigma-Aldrich, Germany) was added in a 1:500 dilution and the sections were kept at 4 degrees overnight. On staining day 2, after 3x10min washing with 0.1% Triton-PBS, the sections were incubated with the secondary antibody solution containing 1% donkey serum, 1:500 Ab'' (anti-rabbit Alexa 568, A-10042 Invitrogen, USA), 1:250 NeuroTrace 435 (N21479 Invitrogen, USA) and 0.1% Triton in PBS. After 2h in room temperature, sections were washed again with PBS 3x10 min, mounted on gelatin-covered glass slides and coverslipped for later observation. For the GFAP and Iba1 staining of brain sections the same process was followed but the primary antibodies were goat anti-GFAP (ab53554, abcam USA) in 1:750 dilution and rabbit anti-Iba1 (019-19741, FUJIFILM Wako Pure Chemical Corporation USA) in 1:750 dilution. The secondary antibodies used were donkey anti-goat Alexa 555 (A-21432 Invitrogen, USA) for the GFAP labeling and donkey anti-rabbit Alexa 488 (A-21206, Invitrogen, USA) for the Iba1 labeling.

Global Ischemia mouse model

Operation

Global cerebral ischemia was induced as previously described [25] [26]. Briefly, 32 6- to 8-week-old male C57BL/6N mice with a body weight of 20 to 24g (Charles River Laboratories, Sulzfeld, Germany) were anesthetized with a combination of Buprenorphine (0.1mg/kg, Essex Pharma, Germany) and 2% isoflurane (Halocarbon Laboratories, Peachtree Corners, GA) in 50% O_2/50% N_2. Body temperature was tightly controlled using a feedback controlled heating pad (FHC, Bowdoinham, USA). Regional cerebral blood flow (rCBF) was continuously monitored over the right hemisphere with a laser Doppler perfusion monitor (Periflux 4001 Master, Perimed, Sweden). The neck was opened and both common carotid arteries were exposed. A catheter was placed in the left common carotid artery and then both common carotid arteries were occluded with atraumatic clips. After seven and a half minutes the clips were removed and 50 µl of GA (Stock solution 3,92M in water, pH adjusted to 7 with NaOH, end

bioRxiv preprint doi: https://doi.org/10.1101/2020.11.24.396051; this version posted November 24, 2020. The copyright holder for this preprint (which was not certified by peer review) is the author/funder, who has granted bioRxiv a license to display the preprint in perpetuity. It is made available under aCC-BY-NC-ND 4.0 International license.

concentration in PBS 120mM, N=7 mice) or PBS (0.01M, N=9) were injected into the left common carotid artery. Thereafter, the catheter was removed, the incision was sutured and animals received 100 µl of Carprofen (1mg/ml) s.c. for postoperative analgesia. Sham-operated mice (N=16) underwent the same surgical procedure without carotid clipping. Animals were randomly and blindly allocated to the respective treatment group shortly before injection of GA or PBS.

Animal fixation, tissue processing & quantification

One week after global ischemia, mice were re-anesthetized and transcardially perfused with 4% PFA. Brains were extracted, dehydrated, embedded in paraffin, cut into 4 µm thick coronal sections, and stained with cresyl violet for neuronal cell counting. Intact neurons in the hippocampal CA1a, CA1b, CA2, and CA3 subregions were counted using Image J (National Institutes of Health, Bethesda, MD) by an investigator blinded to the treatment of the mice. Three sections per mouse were assessed for this analysis.

Functional tests

Besides histological damage, MCAo is known to induce deficits in motor function, including motor coordination, balance and muscle strength with mice showing preference for using the non-affected limb [27]. Therefore, we performed different functional tests to assess such deficits.

Pole test

The pole test is a method for simple motor function evaluation [28] [29] and was performed on day 8 post-MCAo operation after preoperative training. Animals were placed on top of a 10mm-diameter, 55cm-long vertical pole and were observed as they turned around and descended the pole (snout first). Scoring began when the animal started the turning movement. The time to make a full 180° turn (time to turn) and latency to reach the ground (time to come down) was recorded. Mice had to successfully perform the descend 3 times. Trials where mice took longer than 5s to turn or longer than 20s to come down were excluded. Pausing was also an exclusion criterium.

Gait analysis

For gait analysis the CatWalk (Noldus Information Technology) automated, computer-assisted system was used, that is often implemented to assess locomotion defects in stroke mouse models [30]. The Cat Walk apparatus contains a long elevated glass runway platform that is

bioRxiv preprint doi: https://doi.org/10.1101/2020.11.24.396051; this version posted November 24, 2020. The copyright holder for this preprint (which was not certified by peer review) is the author/funder, who has granted bioRxiv a license to display the preprint in perpetuity. It is made available under aCC-BY-NC-ND 4.0 International license.

fluorescently illuminated from the inside and the light is reflected to the direction of the floor when pressure (weight) is applied on top. A camera is mounted underneath the glass platform to record the walking pattern. At the beginning of the experiment, the animals' home cage was placed at one end of the platform and mice were placed at the opposite side in order to voluntarily walk across the platform towards their home cage. Analysis was performed using CatWalk XT 10.5 Software which visualizes the prints and calculates statistics regarding their dimensions and the time and distance ratios between footfalls. For a trial to be considered successful, the animal should not have a speed variation larger than 60% and the run should be uninterrupted (no stopping on the runway). Unsuccessful trials were repeated until 3 successful trials were reached. Before baseline acquisition, mice were preoperatively trained for 3 days with the CatWalk system in (three runs per day). Post-stroke acquisition was performed on day 10 post-ischemia.

Corner test

The corner test, developed for measuring sensorimotor asymmetries after unilateral corticostriatal damage, was performed on day 12 post-stroke [31]. It is composed of two connected cardboard walls forming a corner of approximately 30°. At the junction of the walls, a small opening is left to motivate the mice to reach deep into the corner. At the beginning of the test, each animal is placed halfway from the corner, facing it. As the mice walk into the corner their vibrissae are stimulated and as a response they rear and turn to either side (left or right). Each session lasted 10 min. and the turns in each direction were recorded. The Laterality Index (LI) was calculated using the following formula as described previously by Balkaya and Endres, 2010 [32]:

$$LI = \frac{TL-TD}{TD+TL}$$

where TL: Turn Left (stroke affected side), TD: Turn Right (non-affected side)

MRI

Ischemic lesion size was quantified using magnetic resonance imaging (Bruker 7T PharmaScan 70/16) day 1 and 13 after MCAo. Analyze software (AnalyzeDirect, Overland Park, USA) was implemented to manually define the infarct size. Following focal ischemia, a common pathology observed is cerebral edema which has to be accounted for, when measuring the infarct size.

bioRxiv preprint doi: https://doi.org/10.1101/2020.11.24.396051; this version posted November 24, 2020. The copyright holder for this preprint (which was not certified by peer review) is the author/funder, who has granted bioRxiv a license to display the preprint in perpetuity. It is made available under aCC-BY-NC-ND 4.0 International license.

Lesion volumes were determined by computer-aided manual tracing of the lesions and corrected for the space-occupying effect of brain edema using the following equation [33]:

$$\%HLVe = \frac{2*LVe}{HVc+HVi} * 100$$

where %HLVe is the edema–corrected lesion volume as a percent of the hemispheric volume, HVc and HVi represent the contralateral and ipsilateral hemispheric volume and LVe stands for edema corrected lesion volume.

Stereological evaluation

For the stereological analysis we used a Zeiss AxioImager I (Zeiss, Göttingen, Germany) and the StereoInvestigator Software 8.0 (MicroBrightField, Magdeburg, Germany). To calculate the infarct volume and the number of surviving (NeuN positive) neurons on this infarct we used a series of 60μm-thick brain sections, sampling every 360 μm, starting from the first one with an obvious infarct (as defined by the Neurotrace 435 staining) and ending with the last one with an obvious infarct. Using the optical fractionator workflow provided by the software, the sampled sub-volumes were extrapolated to arrive at an estimate of the entire cell population. A virtual space called an optical dissector was implemented and counting rules were followed to prevent overestimating. On each brain section we separately outlined the infarcted area that was still there (infarct volume) and the infarcted area that was missing due to cyst formation after necrosis (ischemic core volume). We then estimated the neuronal density within the infarcted volume, the neuronal density on the intact contralateral (control) side, as well as the ratio between the two densities.

GFAP and Iba1 fluorescence signal analysis

3 sections per brain were imaged using an Apotome .2 fluorescence microscope (Zeiss, DE), 4x objective and mosaic function. The images were then analyzed in image J (National Institutes of Health, Bethesda, MD). Briefly, after background removal, the ischemic area defined by high Iba1 signal was outlined and the mean fluorescence intensity of both Iba1 and GFAP signal on that area was measured. The rest of the ipsilateral to ischemia hemisphere (ischemic area and ventricles excluded) was also outlined and the mean fluorescence intensity of both markers was measured. Lastly, the contralateral hemisphere (ventricles excluded) was outlined and the mean fluorescence intensity for both markers was measured.

Statistical analysis

bioRxiv preprint doi: https://doi.org/10.1101/2020.11.24.396051; this version posted November 24, 2020. The copyright holder for this preprint (which was not certified by peer review) is the author/funder, who has granted bioRxiv a license to display the preprint in perpetuity. It is made available under aCC-BY-NC-ND 4.0 International license.

All data was analyzed using GraphPad Prism 6 (CA, USA). Statistical tests applied in each case are explained in the figure legends.

RESULTS

GA protects from ischemia-induced neuronal death *in vitro*

The current standard of care for treating acute stroke is the restoration of blood flow to the ischemic region, known as reperfusion. However, this procedure can also induce damage, an effect known as "ischemia-reperfusion injury" [34]. Oxygen-glucose deprivation is a well-established *in vitro* model mimicking ischemia/reperfusion injury, leading to apoptotic and excitotoxicity-induced necrotic and apoptotic cell death [35]. We used this model to determine the neuroprotective properties of GA during ischemia-reperfusion damage. We tested the effect of GA in different concentrations added to the culture media immediately after mimicking 1 hour of ischemia. In order to differentiate between necrosis and apoptosis, we used two different approaches. Necrosis just after the ischemic insult was measured as the ratio between necrotic Propidium Iodide (PI) positive nuclei and the total amount of nuclei stained with DRAQ5 30 min. after OGD compared to normoxic neurons treated with the same concentrations of GA. We observed a significant increase in the PI^+ nuclei in the neuronal cultures that underwent OGD compared to the normoxic cultures (Norm: 0,1324 ± 0,03040; Isch: 0,3687± 0,05995, $p<0.001$) (Figure 1A). Treatment during reperfusion with GA decreased the ratio of necrotic nuclei/total nuclei compared to ischemia with vehicle, the highest effect was observed with the 20mM concentration (Isch+20mM: 0,1564 ± 0,008922, $p<0.001$). The same concentrations of GA did not have any effect in the normoxia group when compared to normoxia vehicle even with the highest concentrations (Norm+20mM: 0,1083 ± 0,02140, $p>0.05$). We then looked at the number of NeuN+ neurons at 72h post-OGD in order to evaluate the total cell death (combination of necrosis that occurs at early stages and apoptosis that takes place at later stages after OGD). As shown in figure 1, OGD resulted in the loss of 76% of $NeuN^+$ cells when compared to normoxia (Norm: 1092 $NeuN^+$ cells in 10 fields/well ± 284,0; Isch: 255,3 ± 35,32, $p<0,05$). Treatment with 10mM and 20 Mm GA immediately after OGD exerted a clear protection, increasing the number of surviving neurons to levels comparable to normoxia (Isch+10mM GA: 1230 ± 154,8, p=0,6930; Isch+20mM GA: 1404 ± 422,5, p= 0,5735). There was no significant difference in neuronal survival between 10mM and 20mM GA treatment (p= 0,7182). These results show that treatment with 10mM or higher GA concentrations during reperfusion was enough to rescue neurons from ischemia-induced cell death following OGD.

bioRxiv preprint doi: https://doi.org/10.1101/2020.11.24.396051; this version posted November 24, 2020. The copyright holder for this preprint (which was not certified by peer review) is the author/funder, who has granted bioRxiv a license to display the preprint in perpetuity. It is made available under aCC-BY-NC-ND 4.0 International license.

Unilateral intra-arterial administration of GA during reperfusion protects against neuronal death in the ipsilateral CA1 region of the hippocampus during global ischemia in mice

Based on these results, we wanted to evaluate the effect of GA on a well-established *in vivo* model of global ischemia which occurs in clinical situtations that induce a pronounced drop in the oxygen or blood supply to the brain leading to anoxic/hypoxic brain damage (e.g. heart infarcts, heart arrythmias, sudden and prolongued drop in the blood pressure or insufficient oxygen/blood supply in prolonged or complicated labour). For that purpose, we used the mouse model of global ischemia as previously described [25] [26] to test the effect of PBS (vehicle) or GA injected in the left carotid artery during reperfusion (Figure 2A-C). Global ischemia resulted in neuronal death in the hippocampal CA1-region of both hemispheres in the vehicle group (sham vs vehicle right: mean diff.= 32,78, $p<0.001$; sham vs vehicle left: mean diff.=27,67, $p<0.01$) (Figure 2D) Interestingly, the injection of GA in the left carotid artery during reperfusion resulted in a significant increase in neuronal survival in the left CA1 when compared to the contralateral (right) CA1, where a significant loss of neurons was observed when compared to sham animals (sham vs GA right: mean diff.= 45,71, $p<0.0001$). Remarkably, the number of surviving neurons in the left CA1 (ipsilateral to the GA injection did not differ from the sham group (sham vs GA left: mean diff.= 7,429, $p>0.05$).

Intraperitoneal GA treatment during reperfusion improves the histopathological and functional outcome in the MCAo mouse model

To further confirm the observed neuroprotective effects of GA in another, relevant *in vivo* model, we tested its effect in the Middle Cerebral Artery Occlusion-MCAo mouse model, the most commonly used model in stroke studies [36]. Our experimental timeline is described in detail in Figure 3A.

As illustrated in supplementary Figure S1A, the number of surviving mice until the endpoint (14 days post-ischemia) was higher in the GA treated group compared to vehicle mice but the difference was not statistically significant (94.44% vs. 76.47%, Mantel-Cox test: Chi square= 3.411, $p=0.181$) while all sham-operated mice survived throughout the experiment. We observed that mortality occurred only in mice with larger infarcts (above 18% of the hemispheric volume) (Figure 3Bi). Therefore, we analyzed survival in large infarcts. In this case, a Mantel-Cox survival analysis showed that GA significantly increased mouse survival. More specifically, while 66% of the vehicle-treated mice died by day 5, only 14,2% of the GA-treated died by that

bioRxiv preprint doi: https://doi.org/10.1101/2020.11.24.396051; this version posted November 24, 2020. The copyright holder for this preprint (which was not certified by peer review) is the author/funder, who has granted bioRxiv a license to display the preprint in perpetuity. It is made available under aCC-BY-NC-ND 4.0 International license.

time (Chi square=6.215, p=0.0447) (see Figure 3Bii). Moreover, GA treatment had no effect on the ischemia-induced weight loss compared to vehicle and showed only a tendency to improve the general health score but the difference was not statistically significant (figure S1B, C). The body surface temperature was not influenced by ischemia or treatment (figure S1D).

According to our MRI observations on day 1 post-MCAo, GA did not significantly alter the total lesion size compared to vehicle (see figure S2). However, GA treatment had a strong effect on the evolution of the lesion size. As can be observed in Figure 3C and D there was a significant infarct size reduction at day 13 post-ischemia compared to day 1 post-ischemia (paired t-test, p= 0.0004). On the contrary, no significant reduction was observed in the vehicle group (Figure 3E; paired t-test, p= 0,0914). Therefore, GA significantly improved the late outcome after ischemia.

With regards to the motor function assessment, the pole and catwalk tests did not detect any significant differences between sham- and MCAo-operated mice, independently of treatment (figures S3, S4 and supplementary table 1).

On the other hand, the corner test performance was positively influenced by GA. As shown in Figure 3F, ischemia without treatment significantly increased the laterality index of the corner test compared to sham (0.48± 0.242 vs -0.065 ± 0.172 p=0.0064, respectively). In contrast, the LI in the GA treated group was not significantly different from the sham operated group (0.26 ±0.451, p= 0.1042). Therefore, GA treatment reduced the ischemia-induced sensorimotor asymmetry to levels resembling the performance of the sham group. Following that, we examined the relationship between infarct size and performance on the corner test. In principle, large infarcts should lead to bigger impairments and higher LI values. Indeed, this was the case for vehicle treated mice (Figure 3G). However, this correlation was not found in the GA treated group. This finding again suggests that GA improved the functional outcome especially in animals with larger ischemic lesions.

Following the aforementioned *in vivo* tests, we performed histological analysis on day 14 post-operation. We used Neurotrace (a Nissl- based fluorescence staining) to differentiate between healthy and infarcted tissue and NeuN immunostaining to identify and count surviving neurons in this area. Nissl substance redistributes within the cell body in injured or regenerating neurons, providing a marker for the physiological state of the neuron, thereby identifying the damaged area but cannot differentiate between the part of the penumbra that survived and is regenerating and the part that died within the next days after stroke in a patched manner due to apoptosis

bioRxiv preprint doi: https://doi.org/10.1101/2020.11.24.396051; this version posted November 24, 2020. The copyright holder for this preprint (which was not certified by peer review) is the author/funder, who has granted bioRxiv a license to display the preprint in perpetuity. It is made available under aCC-BY-NC-ND 4.0 International license.

and did not liquefy and detach. In any case, one can assume that after 14 days the ischemic core has been partially liquified due to liquefactive necrosis [5] [37] [38] and is detached during our brain slice preparation, considered as "missing tissue" (Figure S5). Stereological analysis (Stereo Investigator, MBF) provided an estimation of cell density inside the Neurotrace$^+$ area as well as the volume of the infarct (Figure S5). We could only observe a small non-significant reduction on the number of neurons inside the Neurotrace$^+$ area and GA did not change the size of the total Neurotrace+ area (Figure S6A, D). However, GA treatment led to a non-significant reduction in the volume of the tissue missing within the Neurotrace+ area (sham: 0,00 ± 0,00; vehicle: 1,444 ± 0,3931, p=0,0243; GA: 1,189 ± 0,3230, p=0,0638) (Figure 3F). The missing volume (ischemic core) as measured by stereology was significantly correlated to the infarct volume as measured by MRI on day 13 post-MCAo (Figure S6H) for both the vehicle group (Pearson's r_{veh}= 0.5985, p<0.01) and the GA-treated group (Pearson's r_{GA}= 0.5174; p<0.01). The correlation was significant even when treatment groups were pooled together (Pearson's r= 0.5488; p=0.01).

Lastly, we tested the effect of GA on the stroke-associated increase in astrocytes and microglia in the brain. We used immunohistochemisrty to stain for IBA1 and Glial fibrillary acidic protein (GFAP), well established markers for microglia & macrophages [39] and astrocytes [40], respectively (Figure 4Ai-iii). We measured the fluorescence intensity of these markers in the ischemic area, in the non-ischemic area of the affected hemisphere (ipsilateral) and in the non-affected (contralateral) hemisphere (Figure 4Aiv). As shown in Figure 4Bi and Ci, we observed no significant changes in the amount of microglia or astrocytes inside the ischemic area between sham, vehicle- or GA-treated mice when the brains were pooled independently of their infarct volume as measured by MRI (1-way ANOVA, p=0,1482; p=0,0665, respectively). However, when mice with large infarcts were studied separarely (infarct volume > 18% of the hemispheric volume), the numbers of microglia and astrocytes in the ischemic area were significantly increased in the vehicle group compared to sham (IBA1: mean diff. =-11,31, p<0.05; GAFP: mean diff.= -13,00, p<0.05). Interestingly, the number of microglia and astrocytes in the ischemic area in GA-treated mice were not significantly different to sham (IBA1: mean diff.= -4,354, p>0.05; GFAP: mean diff= -4.354, p>0.05) as shown in Figure 4Bii and Cii. Looking at the ipsilateral, non-ischemic tissue, we found no significant differences in the IBA1 and GFAP fluorescence signal between groups (for both IBA1 and GFAP: 2-way ANOVA, p>0.05). Considering the hemisphere contralateral to the stroke side, we identified a trend for increased IBA1 signal for the vehicle group compared to sham that was very close to reaching statistical significance (mean diff.= -4,531, p= 0,0555), while the levels in the GA group were

bioRxiv preprint doi: https://doi.org/10.1101/2020.11.24.396051; this version posted November 24, 2020. The copyright holder for this preprint (which was not certified by peer review) is the author/funder, who has granted bioRxiv a license to display the preprint in perpetuity. It is made available under aCC-BY-NC-ND 4.0 International license.

very similar to sham (mean diff.=0,4956, p=0,8420). The contralateral GFAP signal did not seem to be significantly affected by MCAo or treatment (2-way ANOVA, p= 0,6408).

DISCUSSION

Glycolic acid has only once been studied in a neurological disease (Parkinson´s disease) [19]. This study revealed that GA increased viability of dopaminergic neurons under exposure to a neurotoxin and the protection is mediated by supporting the mitochondrial activity [19]. The current study is the first to investigate the neuroprotective effects of GA in an *in vivo* setting. Important indications that GA may improve stroke outcomes did not only come from its potential role in regulating apoptosis and protecting mitochondrial function but also from the finding that large GA upregulation is an evolutionary survival strategy of *C. elegans* under metabolically unfavorable environmental conditions [14] [19] [15]. Despite higher organisms, including humans, producing small amounts of GA in their cells [21], they have lost the ability of upregulation during metabolic stress. Therefore, we hypothesized that artificially increasing GA levels in the brain would provide protection under the hypoxic state and metabolic halt induced by ischemic stroke.

In order to confirm our hypothesis we tested these substances in *in vitro* (oxygen-glucose deprivation-OGD) and *in vivo* (Global Ischemia and Middle Cerebral Artery Occlusion-MCAo) models of stroke. In our *in vitro* experiments we observed that treatment with GA during reperfusion resulted in a strong protection against OGD-induced neuronal death. We used PI and DRAQ-5 to quantify necrotic cells 30 min. after OGD and staining against NeuN to measure total neuronal loss 72h post-OGD. The implementation of PI to detect necrosis is widely used. PI does not enter healthy or early apoptotic cells with an intact plasma membrane [41] [42] [43] [44]. By combining PI and DRAQ5, which stains all nuclei, the ratio of necrotic cells in culture can be easily determined. The difference to the total amount of neurons 72 hours after OGD allows discriminating between necrotic and apoptotic death. Our results suggest that GA was able to protect against both types of cell death in this model. These strong neuroprotective properties of GA were confirmed in a global ischemia mouse model. Post-ischemia treatment with GA administered intra-arterially and unilaterally in the carotid artery had again a strong effect on neuronal survival in the ipsilateral side of the brain when compared to the opposite hemisphere or the vehicle group. In the MCAo mouse model, i.p. administration of GA led to a non-significant increase in mice survival when compared to the vehicle group. GA treatment also resulted in significant reductions of the infarct volume 13 days post-ischemia, reduced the

bioRxiv preprint doi: https://doi.org/10.1101/2020.11.24.396051; this version posted November 24, 2020. The copyright holder for this preprint (which was not certified by peer review) is the author/funder, who has granted bioRxiv a license to display the preprint in perpetuity. It is made available under aCC-BY-NC-ND 4.0 International license.

size of the missing tissue (liquefactive necrotic area of the infarct core) and improved motor performance.

In the global ischemia mouse model, the specific method used to induce ischemia gave us the advantage of bilateral damage while we applied the substance only in the left carotid artery, unilaterally. In this way, the side ipsilateral to the intra-arterial GA injection was considered as the 'treated side' while the opposite hemisphere was considered as the 'control side' in each animal. As shown in Figure 2C, GA strongly protected from neuronal death in the treated side compared to the opposite, control side, while no such effect was observed in the vehicle group. The lack of effect on the contralateral side indicates that choosing an injection site of high proximity to the damaged brain tissue can lead to better results due to faster distribution and increased accumulation of GA. This is in accordance to previous studies showing that the i.a. application route is more efficient in yielding high concentrations of the administered substance within a region of interest compared to other methods [45] [46] [47] and it also increases BBB permeability 30 to 50-fold in case of hyperosmotic substances for a short but important time window (approximately 6 minutes) [45]. Thus, the ipsilateral intra-carotid administration of GA could have a strong positive influence on the histological and functional outcome of focal stroke.

In order to examine that hypothesis, we aimed to administer GA intra-arterially in a mouse model of focal stroke. We selected the most commonly used and reliable animal model of stroke, the MCAo mouse model. However, due to technical difficulties intra-carotid application was not feasible in the setting that was available. Thus, we decided to test the effects of GA on the outcome of focal ischemia via i.p. administration. In agreement with previous findings in this model, MCAo led to infarcts including large parts of the ipsilateral cortex and striatum as observed by MRI (Figure 3C). The infarct size, independently of the treatment, showed a relatively high variability (Figure S3) ranging from 2 to 40% of the ipsilateral hemisphere volume, while the average was approximately 15%, similar to previous reports [48]. Large variations in ischemic volumes is not uncommon in this animal model and are normally attributed to the cerebral vasculature of C57Bl6 mice. Up to 40% variability is considered acceptable, as determined by a published protocol of standard operating procedures [49]. This variability is due to inter-individual anatomical differences in the Circle of Willis regarding the presence/absence of the ipsilateral posterior communicating artery (PcomA) [50] [51]. In order to avoid this high interindividual variability we used MRI to compare the infarct volume reduction between day 1 and 13 post-ischemia using a paired t-test. GA but not vehicle, significantly improved the

bioRxiv preprint doi: https://doi.org/10.1101/2020.11.24.396051; this version posted November 24, 2020. The copyright holder for this preprint (which was not certified by peer review) is the author/funder, who has granted bioRxiv a license to display the preprint in perpetuity. It is made available under aCC-BY-NC-ND 4.0 International license.

evolution of infarct volume from day 1 to day 13 post-ischemia (Figure 3D and E). Thus, GA induced a better long-term anatomical outcome.

Additionally, we evaluated the effect of GA on the general health status of the mouse. Our dosage (60mg/kg, i.p.) was not expected to be toxic as suggested by studies mentioned in an official FDA report [52]. Indeed, GA treatment was not only non-toxic but even had a positive effect on MCAO-induced mortality when compared to vehicle treatment, when considering only infarct volumes bigger than 18% of the hemispheric volume.

In order to test the influence of GA on the sensorimotor outcome after stroke, among other behavioral tasks we implemented the corner test that was able to detect a significant effect of GA treatment on sensorimotor function after MCAo. According to our results, vehicle-treated mice displayed significantly lower performance compared to sham-operated mice but i.p. administration of GA was able to reduce sensorimotor asymmetry to levels that were not significantly different from sham (Figure 3F). The corner test has consistently been reliable in detecting the influence of various substances on the functional outcome after MCAo as shown by previous studies [53] [54] [55]. Another interesting finding involving the corner test was that only in the GA-treated group, the performance was independent of the infarct volume. This gave us an indication that GA offers protection despite the size of ischemic area, possibly by increasing the number of surviving neurons inside this area or by supporting their plasticity.

In order to further investigate this, we quantified the number of surviving neurons in the ischemic area. In this regard, it has to be taken into consideration that at 14 days post-stroke the ischemic core is undergoing a liquefactive transformation [37] [38] and can detach from the tissue during immunohistochemical processing depending on the degree of transformation and fragility of the tissue. This missing tissue should not be confused with the enlargement of the lateral ventricles. In this study we observed missing tissue even in regions posterior to the end of the LV (approximately at bregma between -3.7 and -3.15). In this region, the pyramidal cell layer of the hippocampus and the CA1 region was completely missing (example in Figure S5D). The significant positive correlation between ischemic volume and the volume of missing tissue also points in this direction, as unrelated artefacts would not have shown any correlation. Therefore, the remaining Neurotrace+ surrounding tissue can be considered part of the penumbra with regenerating neurons showing a higher Neurotrace signal when compared to the rest of the brain [56] [57] [58] [59]. The evaluation of neuronal survival in the remaining Neurotrace+ tissue using stereology showed no significant differences in cell density between groups. Moreover, the cell density in the ischemic versus intact hemisphere was reduced but

bioRxiv preprint doi: https://doi.org/10.1101/2020.11.24.396051; this version posted November 24, 2020. The copyright holder for this preprint (which was not certified by peer review) is the author/funder, who has granted bioRxiv a license to display the preprint in perpetuity. It is made available under aCC-BY-NC-ND 4.0 International license.

not significantly different in any of the group. This might be due to the fact that NeuN protein is not expressed only by neurons but also by astrocytes [60] [61] and numbers of astrocytes are known to be increased after stroke in the infarct and peri-infarct area [62] [63] [64]. Alternatively, it is possible that the neuronal loss in the penumbra is 'patchy' as described previously [65] [66] and it's therefore hard to detect as significant reduction in cell density. Although GA did not alter the cell density in the infarct site, it reduced the ischemic core volume in contrast to vehicle (GA group not significantly different from sham) which could contribute to the improved functional outcome we saw after stroke. Thus, our observation that the core in the GA group is reduced suggests that GA might have initially increased the salvaged penumbra area.

As ischemia induces a strong immune response in the human brain, including an increase in the astrocyte and microglia levels [60], we also tested whether GA had an effect on the amount of astrocytes and microglia in the mouse brain after MCAo. When evaluated independently of the infarct volume, no significant difference in the fluorescence marker levels of astrocytes or microglia between vehicle and GA treated groups was detected. However, as functional and survival data indicated, when analyzed independently, larger infarcts were associated with a significantly increased GFAP and Iba1 signal in the vehicle group but not in the GA group when compared to sham. We did not observe this difference in smaller infarcts, where GFAP and Iba1 signals were equally increased in vehicle and GA treated mice. The regions that are mainly affected in these two cases could explain this difference in the results between small and big ischemic volumes. In brains with smaller infarct volumes the mainly affected area was the striatum, which is the primary target of MCA supply and is known to have very low collateral density [67] [68] [69]. The striatum is consistently infarcted even in mild strokes (30 min MCAo) while for severe MCAO (120 min) the necrotic area expands over the striatum to large fraction of the surrounding cortex, where a penumbra area is observed due to a better collateral irrigation [58]. Moreover, as a result of MCAo the striatum displays certain metabolic changes that are representative of the infarct core rather than the penumbral area [69]. Our results suggest three possibilities: i) GA improves the functional outcome after stroke by reducing the persistent astrocyte and microglia increase triggered by ischemia (both in the ischemic and remote, non-ischemic areas which is known to be detrimental to recovery [70] [71] [72] [73]; ii) GA reduces ischemic damage by reducing necrosis and apoptosis, thereby salvaging a higher fraction of the penumbra and core and the associated release of pro-inflammatory molecules from dying cells (which is supported by our ischemic core and infarct volume evolution data), and as a result the inflammatory reaction is decreased or iii) a combination of both. Based on the *in vitro* results, we think that the second option is the most likely. Although primary cortical

bioRxiv preprint doi: https://doi.org/10.1101/2020.11.24.396051; this version posted November 24, 2020. The copyright holder for this preprint (which was not certified by peer review) is the author/funder, who has granted bioRxiv a license to display the preprint in perpetuity. It is made available under aCC-BY-NC-ND 4.0 International license.

neuronal cultures may have some remaining glia cells, even with the use of B27 supplement that reduces their amount, it is highly unlikely that, in this model, reducing the inflammatory response through GA would lead to the protection observed. Even less likely in the case of the observed protection against necrosis, that occured just minutes after the OGD insult. At such an early time-point the presence of an inflammatory response is highly unprobable. However, this should be further investigated. Additionally, it cannot be excluded that functional improvement is mediated by increased plasticity, which would not be detected by our NeuN+ quantification. GA might be able to enhance the neuronal plasticity which has been shown to be induced as response to stroke [74] [75] [76], however further research is required to confirm this hypothesis. The underlying molecular mechanism by which GA exerts its neuroprotective effects it´s being currently investigated in an ongoing study by our group. Preliminary data suggests that GA reduces the intracellular calcium (which is increased upon stroke) and preserves normal mitochondrial function (which is also deteriorated after stroke).

With the exception of the survival rate in large infarcts, in the MCAo model we generally identified significant differences between the vehicle and sham groups while the GA group was more similar to (or not-significantly different from) sham. However, no statistically significant differences between GA and vehicle were observed. We believe that this is due to the aforementioned high inter-individual variability in the infarct volume within the same group in this model and to the artefact caused by the inclusion of data from mice with large infarcts that survived in the GA group but did not in the vehicle group. This introduces an inequality difficult to solve and this was also one of the reasons to analyse small and large infarcts separately.

Comparing the results from our two different *in vivo* models, we found stronger histological evidence for GA neuroprotection in the global cerebral ischemia mouse model when compared to the MCAo mouse model, even if some positive functional and macroscopic effects where observed in the latter. Intra-arterial application instantly increases local concentrations of GA in the treated hemisphere resulting in an ipsilateral higher cell viability in the global ischemia model. In the case of the MCAo model, the neuronal density in the penumbra was not significantly decreased in the vehicle or GA-treated groups when compareds to sham, probably due to the aforementioned patchy cell death in this region. Thus, it is difficult to asses whether GA was protective at the histological level. However, we did observe a positive effect in the survival and in the reduction of the infarct volume with i.p. administration. Possible explanations

bioRxiv preprint doi: https://doi.org/10.1101/2020.11.24.396051; this version posted November 24, 2020. The copyright holder for this preprint (which was not certified by peer review) is the author/funder, who has granted bioRxiv a license to display the preprint in perpetuity. It is made available under aCC-BY-NC-ND 4.0 International license.

for the difference in the outcome are i) different ischemia times and ii) different routes of administration implemented in each model.

Altogether, our results suggest that GA treatment has a strong neuroprotective effect when administered at high concentrations inmediately after the ischemic insult. Also, our results suggest that GA may increase neuronal plasticity responses after stroke. These results need to be further investigated as our study has certain limitations, such as: i) all experiments were done on young male mice, so the effect on different sex and/or age still needs to be tested, ii) mouse strains (C57BL/6N vs C57BL/6J), ischemia duration, time-points for analysis and treatment administration routes differed between the two *in vivo* models and therefore this can create a discrepancy in their sensitivity, iii) while both models mimic the mechanical thrombectomy occurring in the clinical setting, none of them mimics the pharmacological thrombolysis which is clinically achieved using recombinant tissue plasminogen activator (rTPA) and possible interactions between GA and rTPA should be ruled out. If confirmed in other animal models of media infarct in which the intra-arterial administration of the substances together with rtPA is possible [77] [78], this would have important implications in the clinical setting as it would be highly applicable in human stroke patients, where GA could be added during the reperfusion therapy acutely after stroke.

AUTHOR CONTRIBUTIONS

FP-M designed and coordinated the study. FP-M, IR-A and CF-S designed the OGD experiments. FP-M and NP designed the Global Cerebral Ischemia experiments. AM, KW and FP-M designed the MCAo experiments. IR-A and YD performed the OGD *in vitro* experiments, including imaging and analysis. NP coordinated the Global Cerebral Ischemia experiments. UM performed the Global Cerebral Ischemia operations and assessment of neuronal survival. AM, DB and KW coordinated the MCAo experiments. DB, KW and CD performed the MCAo operations and GA administration. LW, MA and AC performed the MRI-infarct size assessment, functional tests and their analysis for the MCAo mouse model. AC and YD performed the histological processing and analysis of the MCAo brain tissue. AC performed the stereological analysis of the MCAo brains. FP-M, AM, NP, AC, DB and UM wrote the manuscript. All other authors critically revised and corrected the manuscript.

AKNOWLEDGEMENTS: This work was funded by the Deutsche Forschungsgemeinschaft (DFG, German Research Foundation) under Germany's Excellence Strategy within the

bioRxiv preprint doi: https://doi.org/10.1101/2020.11.24.396051; this version posted November 24, 2020. The copyright holder for this preprint (which was not certified by peer review) is the author/funder, who has granted bioRxiv a license to display the preprint in perpetuity. It is made available under aCC-BY-NC-ND 4.0 International license.

framework of the Munich Cluster for Systems Neurology (EXC 2145 SyNergy – ID 390857198) and by the German Ministry for Economy and Energy with an EXIST-Forschungstransfer Grant (GLYMIPRO-FKZ03EFLBY173).

CONFLICT OF INTEREST: FP-M has a patent pending on the use of glycolic acid in ischemia. All other authors declare no competing interests.

REFERENCES

1. Collaborators, G.B.D.S., *Global, regional, and national burden of stroke, 1990-2016: a systematic analysis for the Global Burden of Disease Study 2016.* Lancet Neurol, 2019. **18**(5): p. 439-458.
2. Writing Group, M., et al., *Heart Disease and Stroke Statistics-2016 Update: A Report From the American Heart Association.* Circulation, 2016. **133**(4): p. e38-360.
3. Schaechter, J.D., *Motor rehabilitation and brain plasticity after hemiparetic stroke.* Prog Neurobiol, 2004. **73**(1): p. 61-72.
4. Leigh, R., et al., *Imaging the physiological evolution of the ischemic penumbra in acute ischemic stroke.* Journal of cerebral blood flow and metabolism : official journal of the International Society of Cerebral Blood Flow and Metabolism, 2018. **38**(9): p. 1500-1516.
5. Chung, A.G., et al., *Liquefaction of the Brain following Stroke Shares a Similar Molecular and Morphological Profile with Atherosclerosis and Mediates Secondary Neurodegeneration in an Osteopontin-Dependent Mechanism.* eNeuro, 2018. **5**(5): p. ENEURO.0076-18.2018.
6. Hoyte, L., et al., *The rise and fall of NMDA antagonists for ischemic stroke.* Curr Mol Med, 2004. **4**(2): p. 131-6.
7. Shuaib, A., et al., *NXY-059 for the treatment of acute ischemic stroke.* N Engl J Med, 2007. **357**(6): p. 562-71.
8. Chamorro, A., et al., *Safety and efficacy of uric acid in patients with acute stroke (URICO-ICTUS): a randomised, double-blind phase 2b/3 trial.* Lancet Neurol, 2014. **13**(5): p. 453-60.
9. Lambertsen, K.L., et al., *Microglia protect neurons against ischemia by synthesis of tumor necrosis factor.* J Neurosci, 2009. **29**(5): p. 1319-30.
10. de Bilbao, F., et al., *In vivo over-expression of interleukin-10 increases resistance to focal brain ischemia in mice.* J Neurochem, 2009. **110**(1): p. 12-22.
11. Lapchak, P.A., *A critical assessment of edaravone acute ischemic stroke efficacy trials: is edaravone an effective neuroprotective therapy?* Expert Opin Pharmacother, 2010. **11**(10): p. 1753-63.
12. Erkut, C., et al., *Trehalose renders the dauer larva of Caenorhabditis elegans resistant to extreme desiccation.* Curr Biol, 2011. **21**(15): p. 1331-6.
13. Erkut, C., et al., *How worms survive desiccation: Trehalose pro water.* Worm, 2012. **1**(1): p. 61-5.
14. Erkut, C., et al., *Molecular strategies of the Caenorhabditis elegans dauer larva to survive extreme desiccation.* PLoS One, 2013. **8**(12): p. e82473.
15. Erkut, C., et al., *The glyoxylate shunt is essential for desiccation tolerance in C. elegans and budding yeast.* Elife, 2016. **5**.
16. Erkut, C. and T. Kurzchalia, *The C. elegans dauer larva as a paradigm to study metabolic suppression and desiccation tolerance.* Planta, 2015. **242**: p. 389-396.

bioRxiv preprint doi: https://doi.org/10.1101/2020.11.24.396051; this version posted November 24, 2020. The copyright holder for this preprint (which was not certified by peer review) is the author/funder, who has granted bioRxiv a license to display the preprint in perpetuity. It is made available under aCC-BY-NC-ND 4.0 International license.

17. Gourdin, M. and P. Dubois, *Impact of Ischemia on Cellular Metabolism*, in *Artery Bypass*. 2013.
18. Sullivan, J., *Bad Things Happen in Ischemia*. 2008, WSU Emergency Medicine Cerebral Resuscitation Laboratory.
19. Toyoda, Y., et al., *Products of the Parkinson's disease-related glyoxalase DJ-1, D-lactate and glycolate, support mitochondrial membrane potential and neuronal survival.* Biol Open, 2014. **3**(8): p. 777-84.
20. Thornalley, P.J., *Glyoxalase I--structure, function and a critical role in the enzymatic defence against glycation.* Biochem Soc Trans, 2003. **31**(Pt 6): p. 1343-8.
21. Lee, J.Y., et al., *Human DJ-1 and its homologs are novel glyoxalases.* Hum Mol Genet, 2012. **21**(14): p. 3215-25.
22. Sciarretta, C. and L. Minichiello, *The preparation of primary cortical neuron cultures and a practical application using immunofluorescent cytochemistry.* Methods Mol Biol, 2010. **633**: p. 221-31.
23. Au - Engel, O., et al., *Modeling Stroke in Mice - Middle Cerebral Artery Occlusion with the Filament Model.* JoVE, 2011(47): p. e2423.
24. Hata, R., et al., *Evolution of brain infarction after transient focal cerebral ischemia in mice.* J Cereb Blood Flow Metab, 2000. **20**(6): p. 937-46.
25. Smith, M.L., R.N. Auer, and B.K. Siesjö, *The density and distribution of ischemic brain injury in the rat following 2–10 min of forebrain ischemia.* Acta Neuropathologica, 1984. **64**(4): p. 319-332.
26. Sanderson, T.H., et al., *Insulin blocks cytochrome c release in the reperfused brain through PI3-K signaling and by promoting Bax/Bcl-XL binding.* Journal of Neurochemistry, 2008. **106**(3): p. 1248-1258.
27. Balkaya, M., et al., *Assessing post-stroke behavior in mouse models of focal ischemia.* J Cereb Blood Flow Metab, 2013. **33**(3): p. 330-8.
28. Bouet, V., et al., *Sensorimotor and cognitive deficits after transient middle cerebral artery occlusion in the mouse.* Exp Neurol, 2007. **203**(2): p. 555-67.
29. Prinz, V., et al., *Intravenous rosuvastatin for acute stroke treatment: an animal study.* Stroke, 2008. **39**(2): p. 433-8.
30. Caballero-Garrido, E., et al., *Characterization of long-term gait deficits in mouse dMCAO, using the CatWalk system.* Behav Brain Res, 2017. **331**: p. 282-296.
31. Zhang, L., et al., *A test for detecting long-term sensorimotor dysfunction in the mouse after focal cerebral ischemia.* J Neurosci Methods, 2002. **117**(2): p. 207-14.
32. Balkaya, M., et al., *Characterization of long-term functional outcome in a murine model of mild brain ischemia.* J Neurosci Methods, 2013. **213**(2): p. 179-87.
33. Gerriets, T., et al., *Noninvasive quantification of brain edema and the space-occupying effect in rat stroke models using magnetic resonance imaging.* Stroke, 2004. **35**(2): p. 566-71.
34. L, L., W. X, and Y. Z, *Ischemia-reperfusion Injury in the Brain: Mechanisms and Potential Therapeutic Strategies.* Biochemistry & pharmacology : open access, 2016. **5**(4): p. 213.
35. Goldberg, M.P. and D.W. Choi, *Combined oxygen and glucose deprivation in cortical cell culture: calcium-dependent and calcium-independent mechanisms of neuronal injury.* J Neurosci, 1993. **13**(8): p. 3510-24.
36. Carmichael, S.T., *Rodent models of focal stroke: size, mechanism, and purpose.* NeuroRx, 2005. **2**(3): p. 396-409.
37. Nguyen, T.V., et al., *Multiplex immunoassay characterization and species comparison of inflammation in acute and non-acute ischemic infarcts in human and mouse brain tissue.* Acta Neuropathol Commun, 2016. **4**(1): p. 100.
38. Zbesko, J.C., et al., *Glial scars are permeable to the neurotoxic environment of chronic stroke infarcts.* Neurobiol Dis, 2018. **112**: p. 63-78.

bioRxiv preprint doi: https://doi.org/10.1101/2020.11.24.396051; this version posted November 24, 2020. The copyright holder for this preprint (which was not certified by peer review) is the author/funder, who has granted bioRxiv a license to display the preprint in perpetuity. It is made available under aCC-BY-NC-ND 4.0 International license.

39. Sasaki, Y., et al., *Iba1 is an actin-cross-linking protein in macrophages/microglia.* Biochem Biophys Res Commun, 2001. **286**(2): p. 292-7.
40. Pekny, M. and M. Pekna, *Astrocyte intermediate filaments in CNS pathologies and regeneration.* J Pathol, 2004. **204**(4): p. 428-37.
41. Vermes, I., et al., *A novel assay for apoptosis. Flow cytometric detection of phosphatidylserine expression on early apoptotic cells using fluorescein labelled Annexin V.* J Immunol Methods, 1995. **184**(1): p. 39-51.
42. Vermes, I., C. Haanen, and C. Reutelingsperger, *Flow cytometry of apoptotic cell death.* J Immunol Methods, 2000. **243**(1-2): p. 167-90.
43. Faleiro, L. and Y. Lazebnik, *Caspases disrupt the nuclear-cytoplasmic barrier.* J Cell Biol, 2000. **151**(5): p. 951-9.
44. Rieger, A.M., et al., *Modified annexin V/propidium iodide apoptosis assay for accurate assessment of cell death.* Journal of visualized experiments : JoVE, 2011(50): p. 2597.
45. Fenstermacher, J. and J. Gazendam, *Intra-arterial infusions of drugs and hyperosmotic solutions as ways of enhancing CNS chemotherapy.* Cancer Treat Rep, 1981. **65 Suppl 2**: p. 27-37.
46. Dedrick, R.L., *Arterial drug infusion: pharmacokinetic problems and pitfalls.* J Natl Cancer Inst, 1988. **80**(2): p. 84-9.
47. Joshi, S., C.W. Emala, and J. Pile-Spellman, *Intra-arterial drug delivery: a concise review.* J Neurosurg Anesthesiol, 2007. **19**(2): p. 111-9.
48. Doyle, K.P., et al., *Distal hypoxic stroke: a new mouse model of stroke with high throughput, low variability and a quantifiable functional deficit.* J Neurosci Methods, 2012. **207**(1): p. 31-40.
49. Dirnagl, U.a.G., Members of the MCAO-SOP, *Standard operating procedures (SOP) in experimental stroke research: SOP for middle cerebral artery occlusion in the mouse.* Nature Precedings, 2012.
50. Barone, F.C., et al., *Mouse strain differences in susceptibility to cerebral ischemia are related to cerebral vascular anatomy.* J Cereb Blood Flow Metab, 1993. **13**(4): p. 683-92.
51. Fujii, M., et al., *Strain-related differences in susceptibility to transient forebrain ischemia in SV-129 and C57black/6 mice.* Stroke, 1997. **28**(9): p. 1805-10; discussion 1811.
52. Jane Liedtka, M., et al., *Glycolic Acid*

Pharmacy Compounding Advisory Committee

Meeting. 2016, FDA, U.S. Food and Drug Administration: www.fda.gov.
53. Hao, J., et al., *Neuroprotection in mice by NGP1-01 after transient focal brain ischemia.* Brain Res, 2008. **1196**: p. 113-20.
54. Abe, T., et al., *The neuroprotective effect of prostaglandin E2 EP1 receptor inhibition has a wide therapeutic window, is sustained in time and is not sexually dimorphic.* J Cereb Blood Flow Metab, 2009. **29**(1): p. 66-72.
55. Chen, J., et al., *Atorvastatin induction of VEGF and BDNF promotes brain plasticity after stroke in mice.* J Cereb Blood Flow Metab, 2005. **25**(2): p. 281-90.
56. Moon, L.D.F., *Chromatolysis: Do injured axons regenerate poorly when ribonucleases attack rough endoplasmic reticulum, ribosomes and RNA?* Developmental neurobiology, 2018. **78**(10): p. 1011-1024.
57. Bradley, A., et al., *Chapter 13 - Brain*, in *Boorman's Pathology of the Rat (Second Edition)*, A.W. Suttie, Editor. 2018, Academic Press: Boston. p. 191-215.
58. Popp, A., et al., *Identification of ischemic regions in a rat model of stroke.* PLoS One, 2009. **4**(3): p. e4764.
59. Zille, M., et al., *Visualizing cell death in experimental focal cerebral ischemia: promises, problems, and perspectives.* J Cereb Blood Flow Metab, 2012. **32**(2): p. 213-31.

bioRxiv preprint doi: https://doi.org/10.1101/2020.11.24.396051; this version posted November 24, 2020. The copyright holder for this preprint (which was not certified by peer review) is the author/funder, who has granted bioRxiv a license to display the preprint in perpetuity. It is made available under aCC-BY-NC-ND 4.0 International license.

60. Darlington, P.J., et al., *Widespread immunoreactivity for neuronal nuclei in cultured human and rodent astrocytes.* J Neurochem, 2008. **104**(5): p. 1201-9.
61. Gusel'nikova, V.V. and D.E. Korzhevskiy, *NeuN As a Neuronal Nuclear Antigen and Neuron Differentiation Marker.* Acta naturae, 2015. **7**(2): p. 42-47.
62. Barreto, G.E., et al., *Astrocyte Proliferation Following Stroke in the Mouse Depends on Distance from the Infarct.* PLOS ONE, 2011. **6**(11): p. e27881.
63. Sims, N. and W. Yew, *Reactive astrogliosis in stroke: Contributions of astrocytes to recovery of neurological function.* Neurochemistry International, 2017. **107**.
64. Kudabayeva, M., et al., *The increase in the number of astrocytes in the total cerebral ischemia model in rats.* Journal of Physics: Conference Series, 2017. **886**: p. 012009.
65. Ejaz, S., et al., *Cortical Selective Neuronal Loss, Impaired Behavior, and Normal Magnetic Resonance Imaging in a New Rat Model of True Transient Ischemic Attacks.* Stroke, 2015. **46**(4): p. 1084-1092.
66. Baron, J.-C., *Mapping neuronal density in peri-infarct cortex with PET.* Human Brain Mapping, 2017. **38**(11): p. 5822-5824.
67. Block, F., M. Dihné, and M. Loos, *Inflammation in areas of remote changes following focal brain lesion.* Prog Neurobiol, 2005. **75**(5): p. 342-65.
68. Bacigaluppi, M., G. Comi, and D.M. Hermann, *Animal models of ischemic stroke. Part two: modeling cerebral ischemia.* Open Neurol J, 2010. **4**: p. 34-8.
69. Kiewert, C., et al., *Metabolic and transmitter changes in core and penumbra after middle cerebral artery occlusion in mice.* Brain Res, 2010. **1312**: p. 101-7.
70. Yenari, M.A., et al., *Microglia Potentiate Damage to Blood–Brain Barrier Constituents.* Stroke, 2006. **37**(4): p. 1087-1093.
71. Franco, E.C., et al., *Modulation of microglial activation enhances neuroprotection and functional recovery derived from bone marrow mononuclear cell transplantation after cortical ischemia.* Neurosci Res, 2012. **73**(2): p. 122-32.
72. Roy-O'Reilly, M. and L.D. McCullough, *Astrocytes fuel the fire of lymphocyte toxicity after stroke.* Proceedings of the National Academy of Sciences, 2017. **114**(3): p. 425.
73. Liu, Z. and M. Chopp, *Astrocytes, therapeutic targets for neuroprotection and neurorestoration in ischemic stroke.* Progress in neurobiology, 2016. **144**: p. 103-120.
74. Carmichael, S.T., *Plasticity of cortical projections after stroke.* Neuroscientist, 2003. **9**(1): p. 64-75.
75. Ueno, Y., et al., *Axonal outgrowth and dendritic plasticity in the cortical peri-infarct area after experimental stroke.* Stroke, 2012. **43**(8): p. 2221-8.
76. Sanchez-Mendoza, E.H. and D.M. Hermann, *Correlates of Post-Stroke Brain Plasticity, Relationship to Pathophysiological Settings and Implications for Human Proof-of-Concept Studies.* Frontiers in cellular neuroscience, 2016. **10**: p. 196-196.
77. Golubczyk, D., et al., *Endovascular model of ischemic stroke in swine guided by real-time MRI.* Scientific Reports, 2020. **10**.
78. Lundberg, J., et al., *Safety of Intra-Arterial Injection with Tumor-Activated T Cells to the Rabbit Brain Evaluated by MRI and SPECT/CT.* Cell Transplantation, 2017. **26**(2): p. 283-292.

bioRxiv preprint doi: https://doi.org/10.1101/2020.11.24.396051; this version posted November 24, 2020. The copyright holder for this preprint (which was not certified by peer review) is the author/funder, who has granted bioRxiv a license to display the preprint in perpetuity. It is made available under aCC-BY-NC-ND 4.0 International license.

FIGURE LEGENDS

Figure 1 A) GA at all concentrations tested significantly reduced the levels of necrosis at 30 min. post-OGD, as measured by the ratio of PI+ (necrotic) neurons /DRAQ5+ (non-necrotic) neurons. The strongest effect was achieved by 20mM GA. B) GA treatment during reperfusion rescues cortical neurons from 60 min ischemia-induced cell death, up to 72 hours after the insult. Numbers are normalized to normoxia (control). Data are mean ± SEM. Unpaired t-test, n.s non-significant, * means $p< 0.05$, ** means $p<0.01$ and *** means $p<0.001$.

Figure 2 GA increases neuronal survival in the hippocampus of a global cerebral ischemia mouse model. A) Schematic illustration of arteries indicating (arrows) the three positions of transient clipping (7.5 min) for the induction of global ischemia. B) Global ischemia model affects the hippocampus, shown in the red rectangle. C) Neurons were quantified inside the area indicated by the red rectangle (CA1 area). D) Number of neurons quantified after administration of 50µl GA or PBS immediately after ischemia at the moment of reperfusion through a catheter placed in the left carotid artery. The number of surviving neurons in the left CA1 is significantly reduced in PBS-treated animals compared to sham, while no significant difference is observed for the GA-treated group. In contrast, in the right CA1 opposite to the injection site, there is significant neuronal death for both PBS and GA treated animals, underscoring that the neuroprotective effect of GA is local. (1-way ANOVA followed by Dunnetts multiple comparisons test, **p<0,01, ***p<0,001, ****p<0,0001. Data shown as mean± SEM, n_{sham}=16, n_{veh}=9, n_{GA}=7. Ao, aorta; BA, basilar artery; CC, common carotid artery.

Figure 3. GA improves histological and functional outcomes after MCAo. A) Experimental design. Day 0: MCAo or sham operation. Day 1: Early infarct size assessment using MRI. Day 8: Behavioral (motor) assessment using Pole test. Day 10: Gait analysis using Catwalk test. Day 12: Assessment of laterality (preference for non-affected side) using corner test. Day 13: Late infarct size measurement using MRI. Day 14: Brain fixation for further analysis. B i) Survival until post-stroke day 14. Deaths occurred only in mice with infarcts larger than 18% of hemispheric volume). B ii) Considering mice with larger infarcts (>18% of the hemispheric volume) 66% of the vehicle group died by day 5 while only 14,2% of the GA group died by day 5 (Mantel-Cox survival test: Chi square= 6,215, p= 0,0447C; n_{GA}=18, n_{veh}=16, n_{sham}=6) Example MRI image showing the evolution of MCAo-induced infarct in a GA-treated mouse. Upper: Day1 post-ischemia, Lower: Day13 post-ischemia. D) Significant reduction of the infarct size on day 13 compared to day 1 (paired t-test, p= 0.0004, n_{GA}=17). E) Evolution of MCAo-induced infarct in

bioRxiv preprint doi: https://doi.org/10.1101/2020.11.24.396051; this version posted November 24, 2020. The copyright holder for this preprint (which was not certified by peer review) is the author/funder, who has granted bioRxiv a license to display the preprint in perpetuity. It is made available under aCC-BY-NC-ND 4.0 International license.

vehicle-treated mice: Infarct size on day 13 is not significantly different than day 1 (paired t-test, p=0.091, n_{veh}=10. F) Stereological quantification showed that while the vehicle group has significantly higher ischemic core volume than sham (p=0,0243), the difference between GA and sham is not significant (p=0,0638) (unpaired t-test; n_{GA}=17, n_{veh}=10, n_{sham}=5). G) Corner test assesses the preference for the non-affected by ischemia side over the affected side with higher laterality index (LI) indicating higher impairment of the ischemia-affected side. The vehicle-treated group has significantly higher LI compared to sham mice (p=0.0064), while the LI of the GA-treated group is not significantly different from sham (p=0.1042) and the difference between GA-treated and vehicle is also not significant (p=0.3433). 1-way ANOVA followed by multiple comparisons test (n_{GA}=17, n_{veh}=13, n_{sham}=6). H) The functional outcome after MCAo (as measured by the LI index) is not correlated with the infarct size in GA-treated mice (Pearson's r=-0,03202, p=0,9) in contrast to vehicle-treated mice where the correlation is almost significant (Pearson's r=0,5086, p=0,07). n_{GA}=17, n_{veh}=13, n_{sham}=6.

Figure 4. GA mitigates the increase in the amount of astrocytes and microglia in large infarcts after MCAo. A) Fluorescence microscopy images showing the staining for microglia (IBA1, green) and astrocytes (GFAP, red) in a sham brain section (i), as well as a vehicle (ii) and GA brain section with large infarcts. iv) Same brain section as in (iii) indicating the outlines of the different areas in which Mean Fluorescence Intensity (MFI) was measured. B) i) MFI of IBA1 staining in the ischemic area showing no significant differences between groups (1-way ANOVA, p=0,1482) ii) When large infarcts (>18% of hemispheric volume) are analyzed separately, the MFI of IBA1 inside the infarct area is significantly increased in the vehicle group compared to sham (mean diff. =-11,31, p<0.05) while GA did not differ from sham (mean diff.= -4,354, p>0.05). 2-way ANOVA followed by Sidak's multiple comparisons test. iii) The mean fluorescence intensity of IBA1 in the affected (ipsilateral) hemisphere outside the ischemic area was not significantly changed by MCAo (2-way ANOVA, p>0.05) iv) A trend for higher IBA1 MFI in the contralateral hemisphere was observed for the vehicle group compared to the sham, almost reaching statistical significance (2-way ANOVA, p= 0,0555). C)) i) MFI of GFAP staining in the ischemic area showing no significant differences between groups (1-way ANOVA, p=0,0665). ii) When large infarcts (>18% of hemispheric volume) are analyzed separately, the MFI of GFAP inside the infarct area is significantly increased in the vehicle group compared to sham (mean diff.= -13,00, p<0.05) while GA did not differ from sham (mean diff= -4.354, p>0.05) iii) The mean fluorescence intensity of GFAP in the affected (ipsilateral) hemisphere outside the ischemic area was not significantly changed by MCAo (2-way ANOVA, p>0.05. iv) A trend for higher GFAP MFI was observed for the vehicle group compared to the sham and GA

bioRxiv preprint doi: https://doi.org/10.1101/2020.11.24.396051; this version posted November 24, 2020. The copyright holder for this preprint (which was not certified by peer review) is the author/funder, who has granted bioRxiv a license to display the preprint in perpetuity. It is made available under aCC-BY-NC-ND 4.0 International license.

groups but without statistical significance (2-way ANOVA, p>0.05). n_{sham}=3, n_{veh}=6, n_{GA}=7; scale bar ~1000µm.

FIGURES

1

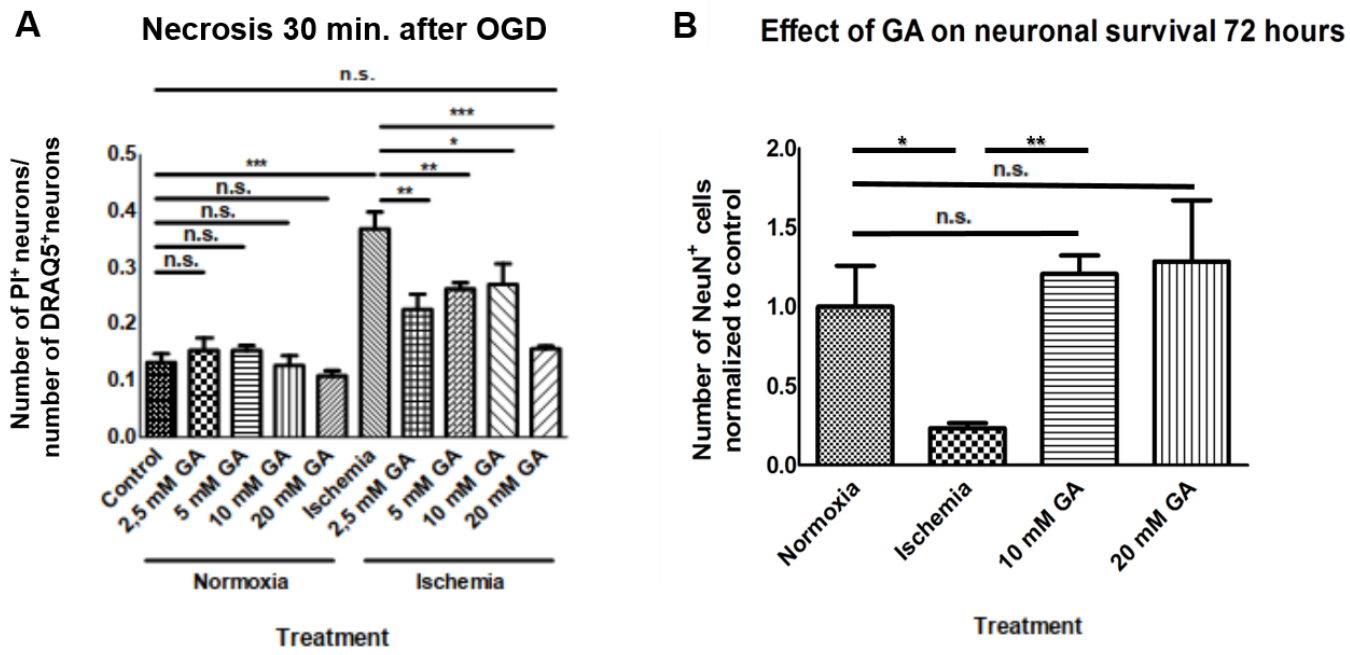

bioRxiv preprint doi: https://doi.org/10.1101/2020.11.24.396051; this version posted November 24, 2020. The copyright holder for this preprint (which was not certified by peer review) is the author/funder, who has granted bioRxiv a license to display the preprint in perpetuity. It is made available under aCC-BY-NC-ND 4.0 International license.

2

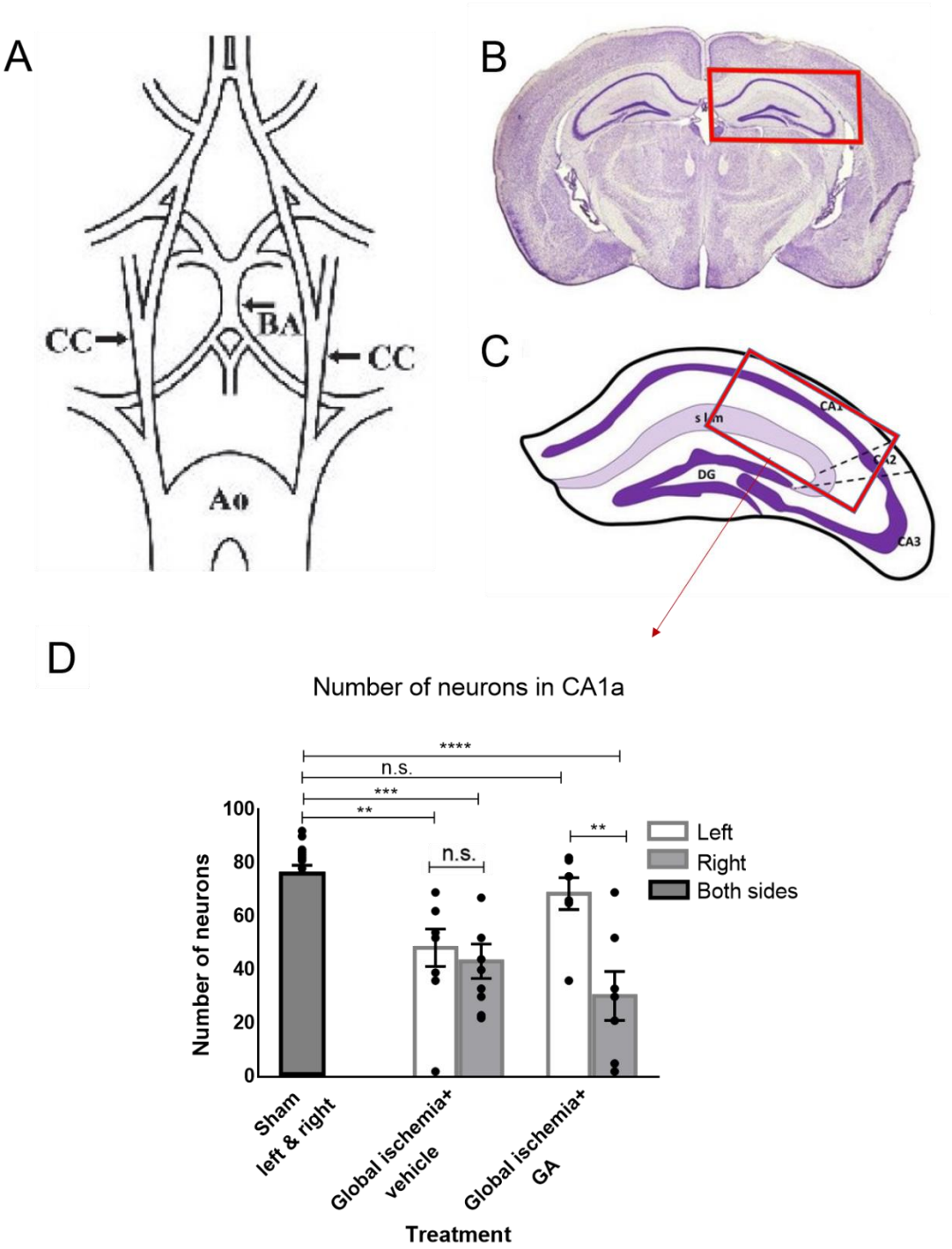

bioRxiv preprint doi: https://doi.org/10.1101/2020.11.24.396051; this version posted November 24, 2020. The copyright holder for this preprint (which was not certified by peer review) is the author/funder, who has granted bioRxiv a license to display the preprint in perpetuity. It is made available under aCC-BY-NC-ND 4.0 International license.

3

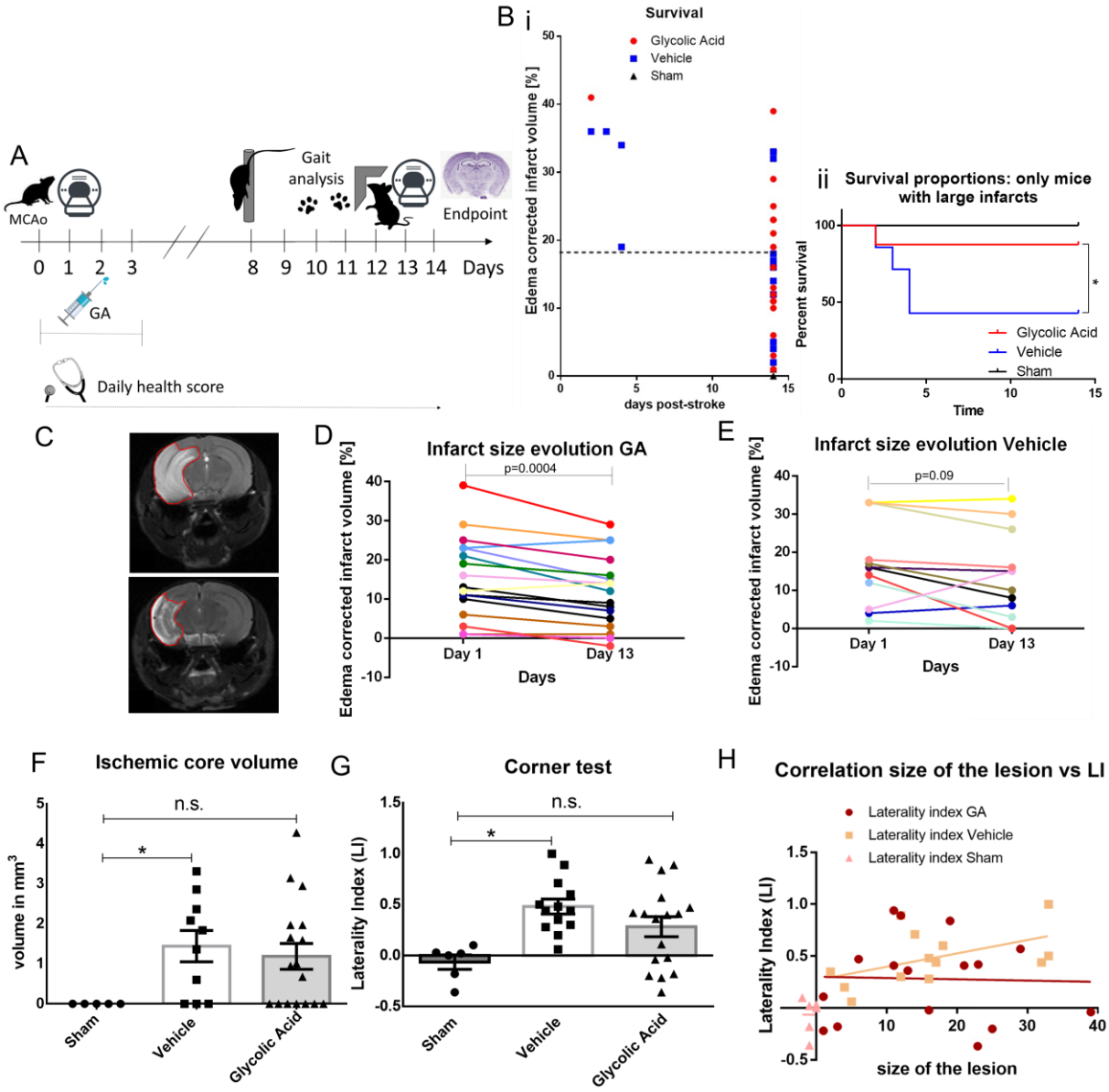

bioRxiv preprint doi: https://doi.org/10.1101/2020.11.24.396051; this version posted November 24, 2020. The copyright holder for this preprint (which was not certified by peer review) is the author/funder, who has granted bioRxiv a license to display the preprint in perpetuity. It is made available under aCC-BY-NC-ND 4.0 International license.
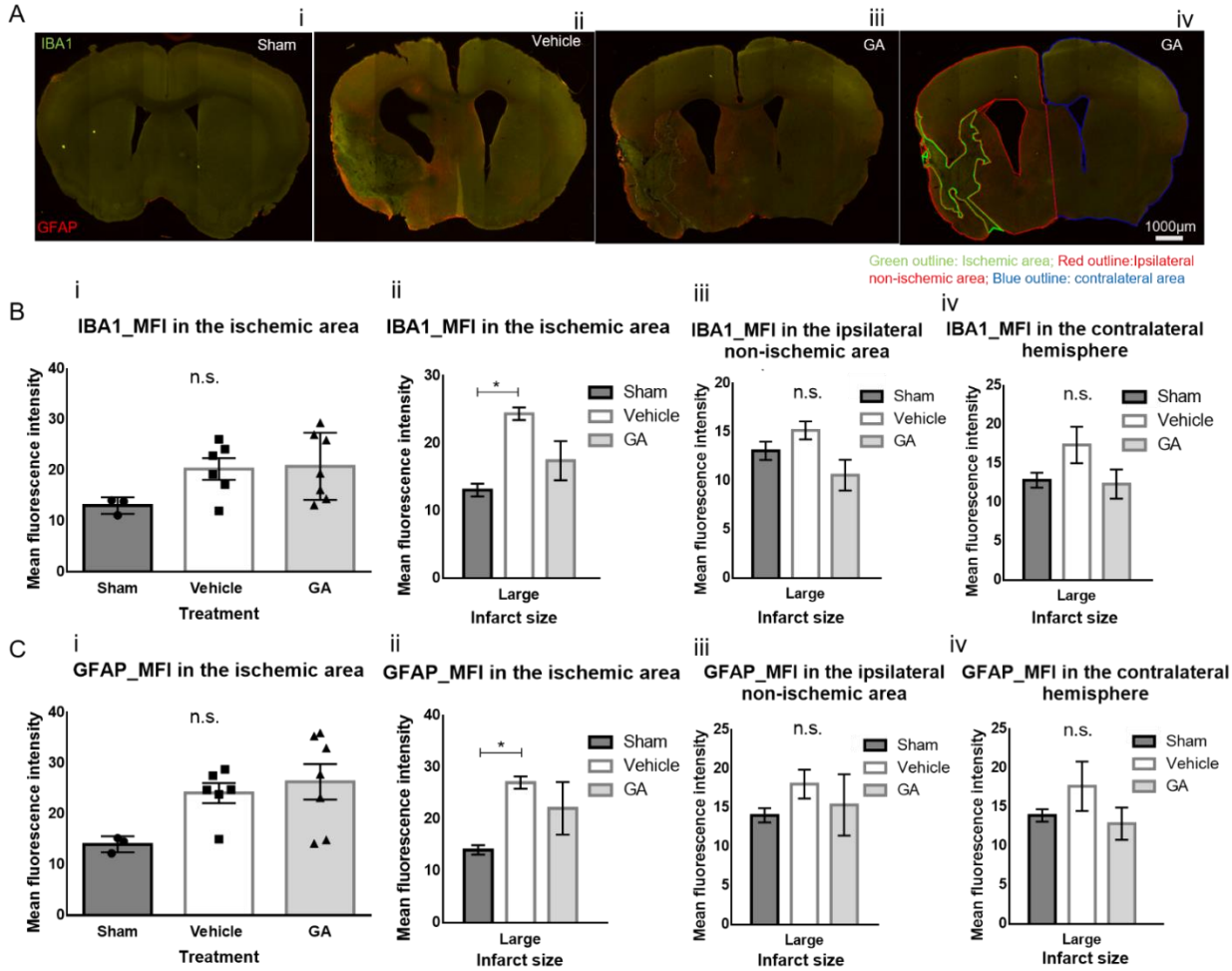
4